IEEE Access
Multidisciplinary | Rapid Review | Open Access Journal

Received April 10, 2020, accepted April 28, 2020, date of publication May 22, 2020, date of current version June 4, 2020.

Digital Object Identifier 10.1109/ACCESS.2020.2996623

A Novel Printed Monopole Antenna With Stepped Impedance Hairpin Resonator Loading

DONG CHEN[1], (Member, IEEE), HONGLIN ZHANG[1], (Member, IEEE), AND CHUNLAN ZHAO[2]

[1]College of Electronic and Optical Engineering and College of Microelectronics, Nanjing University of Posts and Telecommunications, Nanjing 210023, China
[2]13th Research Institute, China Electronics Technology Group Corporation, Shijiazhuang 050051, China

Corresponding author: Honglin Zhang (zhlandhsl@163.com)

This work was supported in part by the National Natural Science Foundation of China under Grant U1636108, and in part by the Nanjing University of Posts and Telecommunications Science Foundation (NUPTSF) under Grant NY2019078.

ABSTRACT In this paper, a novel printed monopole antenna loaded by a stepped impedance hairpin resonator (SIHR) with radial stubs is presented. By loading a SIHR at the bottom of the printed monopole antenna, a printed monopole antenna can be achieved. The resonant frequency of the proposed printed monopole antenna is reduced by the strong coupling between the SIHR and the printed monopole. By utilizing electromagnetic simulation software CST, the antenna is simulated and optimized. After the principle is stated, a sample antenna has been fabricated and measured to verify the predicted performance of our proposed antenna.

INDEX TERMS Printed monopole antenna, near-field resonant parasitic (NFRP), stepped impedance hairpin resonator (SIHR), coupling.

I. INTRODUCTION

With the rapid development of wireless communication technology, how to design a multi-function, low profile and omni-directional wireless communication antenna has become the focus of many engineers [1]. So far, several research reports have been presented on printed monopole antenna [2]. In [2], a part of the radiation patch of the printed monopole antenna is connected to the ground through a shorted pin to realize a printed monopole antenna. In [3], [4], the size of the antenna is reduced by the half-cut method. In [5], [6], a printed monopole antenna is realized by embedding a chip inductor. In [7], the proposed antenna is accomplished by employing a quasi-self-complementarity structure along with a tapered radiating slot.

Recently, researchers have begun to use the near-field resonant parasitic (NFRP) concept to achieve printed monopole antennas [8]. In [9], the NFRP element is a capacitively-loaded loop (CLL) with a varactor to realize printed monopole antenna. In [10], the antenna size is reduced by placing a meander line which acts as an NFRP element near the printed monopole antenna. In [11], a printed monopole antenna is achieved by loading a single fan patch as a NFRP element.

In this paper, a novel printed monopole antenna with stepped impedance hairpin resonator (SIHR) loading is proposed. The SIHR with radial stubs as a NFRP element is electrically coupled to the driven monopole. The strong coupling between the SIHR and the radiator of the driven monopole can reduce the resonant frequency. The stronger the coupling, the lower the resonant frequency, therefore, a novel printed monopole antenna can be realized. Besides, the impedance matching can be easily realized by the coupling between the SIHR and the radiator without any matching circuit. The theoretical analysis and simulated results of the antenna are carefully studied and discussed. Finally, the proposed novel printed monopole antenna is fabricated and measured. The measured results are very close to the predicted ones, which verifies the feasibility of our design method.

II. ANTENNA DESIGN AND DISCUSSION

A. GEOMETRY AND ITS EQUIVALENT CIRCUIT

The configuration of the proposed printed monopole antenna is depicted in Figure 1. It consists of a driven printed monopole antenna and a SIHR located at the back of the

The associate editor coordinating the review of this manuscript and approving it for publication was Diego Masotti.

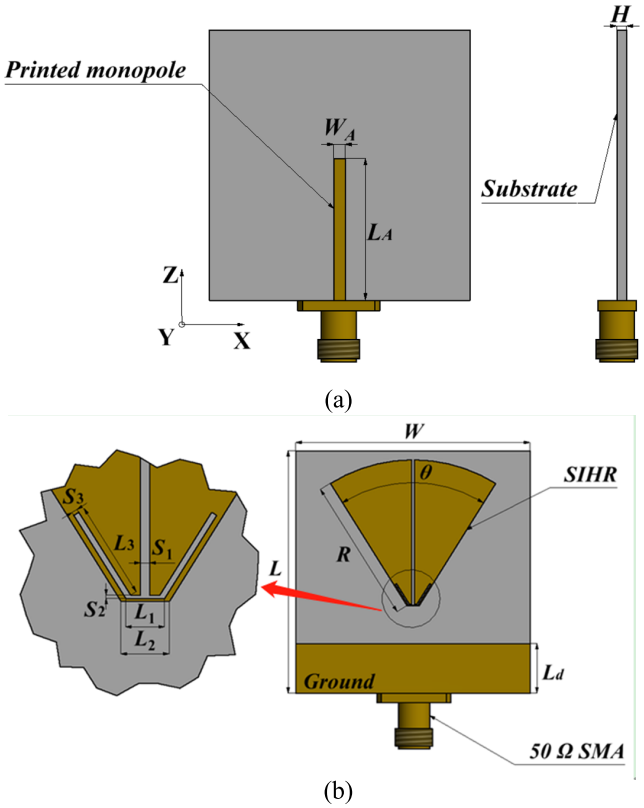

FIGURE 1. Physical layout of the proposed printed monopole antenna. (a) Top view (b) Bottom view.

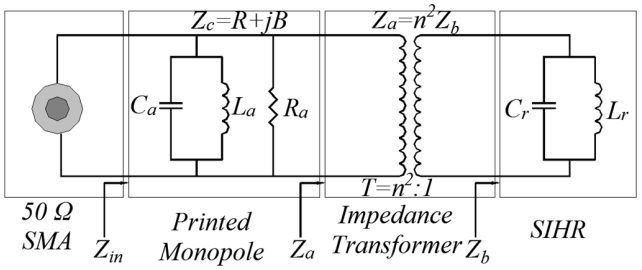

FIGURE 2. Equivalent circuit of the proposed monopole antenna.

antenna. The whole monopole antenna is connected to the 50Ω SMA connector by a microstrip line.

In our design, the whole structure is printed on the substrate Rogers RO4003C. The thickness of the substrate is 0.508 mm, and its relative dielectric constant and loss tangent is $\varepsilon_r = 3.38$, $\tan\delta = 0.0027$, respectively.

In our design, the resonant frequencies of the antenna is reduced by using coupling between the parasitic element and the monopole in the near field of the antenna [12]. Figure 2 shows its total equivalent circuits. Here, the printed monopole

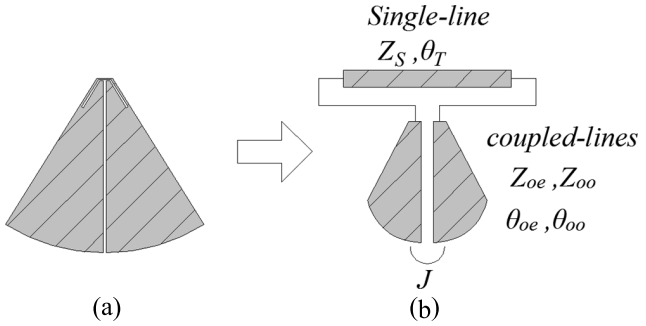

FIGURE 3. SIHR and its equivalent circuit. (a) SIHR structure (b) equivalent circuit.

antenna is equivalent to a lossy parallel resonator with a radiation resistance R_a, inductance L_a, and capacitance C_a. Meanwhile, the SIHR is equivalently represented by a lossless parallel resonator composed of L_r and C_r. As shown in Figure 2, the NFPR element and monopole form a transformer T [13].

B. ANALYSIS OF THE SIHR

Figure 3 shows the equivalent circuit of the SHIR, which is similar to that presented in [14], [15]. It can be analyzed as a parallel circuit composed of a single transmission line and open-ended parallel coupling-line. The even- and odd-mode impedance and corresponding electrical length of coupling-line are denoted by Z_{0e}, Z_{0o}, θ_{oe} and θ_{oo}, respectively. The ABCD-matrix of the coupling-line and single transmission-line are F_1 and F_2, respectively. They can be defined as follows.

$$F_1 = \begin{bmatrix} A_1 & B_1 \\ C_1 & D_1 \end{bmatrix} = \begin{bmatrix} \dfrac{Z_{0e}\cot\theta_{0e}+Z_{0o}\cot\theta_{0o}}{Z_{0e}\cot\theta_{0e}-Z_{0o}\cot\theta_{0o}} & -j\dfrac{2Z_{0e}Z_{0o}\cot\theta_{0e}\cot\theta_{0o}}{Z_{0e}\cot\theta_{0e}-Z_{0o}\cot\theta_{0o}} \\ j\dfrac{2}{Z_{0e}\cot\theta_{0e}-Z_{0o}\cot\theta_{0o}} & \dfrac{Z_{0e}\cot\theta_{0e}+Z_{0o}\cot\theta_{0o}}{Z_{0e}\cot\theta_{0e}-Z_{0o}\cot\theta_{0o}} \end{bmatrix} \tag{1}$$

$$F_2 = \begin{bmatrix} A_2 & B_2 \\ C_2 & D_2 \end{bmatrix} = \begin{bmatrix} \cos\theta_T & jZ_s\sin\theta_T \\ j\sin\theta_T/Z_s & \cos\theta_T \end{bmatrix} \tag{2}$$

The load impedance of an open-ended coupling-line is considered to be infinite. The input impedance Z_b based on the ABCD matrix F_1 and F_2 can be written as:

$$Z_b = \frac{A_1B_2 + A_2B_1}{-(A_1 - A_2)(D_1 - D_2) - (B_1 + B_2)(C_1 + C_2)} \tag{3}$$

$$Z_b = j\left\{\frac{(Z_{oe}-Z_{oo})(Z_{oe}+Z_{oo})Z_s^2\cot\theta_0\sin\theta_T}{[2Z_{0e}Z_{0o}\cot\theta_0 + Z_s(Z_{0e}-Z_{0o})\sin\theta_T] - Z_s\cot\theta_0\,[(Z_{0e}+Z_{0o}) - (Z_{0e}-Z_{0o})\cos\theta_T]^2} + \frac{2\cos\theta_T Z_{oe}Z_{oo}\cot^2\theta_0 Z_s(Z_{oe}-Z_{oo})}{[2Z_{0e}Z_{0o}\cot\theta_0 + Z_s(Z_{0e}-Z_{0o})\sin\theta_T] - Z_s\cot\theta_0\,[(Z_{0e}+Z_{0o}) - (Z_{0e}-Z_{0o})\cos\theta_T]^2}\right\} \tag{4}$$

When $\theta_{oe} = \theta_{oo} = \theta_o$, the impedance Y_b can be simplified as (4), shown at the bottom of the previous page, where, Z_s and θ_T are the characteristic impedance and electrical length of the single transmission line, respectively. In order to calculate Z_{0e} and Z_{0o}, admittance inverter J is introduced [16].

$$Z_{\text{oe}} = Z_0 \times \frac{1 + \text{J}Z_0 \cos \text{ec}\theta_0 + \text{J}^2 Z_0^2}{1 - \text{J}^2 Z_0^2 \cot^2 \theta_0} \tag{5}$$

$$Z_{\text{oo}} = Z_0 \times \frac{1 - \text{J}Z_0 \cos \text{ec}\theta_0 + \text{J}^2 Z_0^2}{1 - \text{J}^2 Z_0^2 \cot^2 \theta_0} \tag{6}$$

In our design, the inverter J is determined by the coupling strength between the microstrip radial stubs, in other words, the gap between the microstrip radial stubs as shown in Figure 3. When the inverter J is determined, Z_{0e} and Z_{0o} can be calculated from the formulas (5) and (6) by specifying electrical length θ_o.

Where, Z_0 and θ_0 are the characteristic impedance and electrical length of the microstrip radial stub, respectively. Using the empirical formula [17, 18], the parameters Z_0 and θ_0 can be calculated.

C. ANALYSIS OF THE MONOPOLE ANTENNA

Now, we analyze the equivalent circuit of the proposed printed monopole antenna shown in Figure 2. Based on the analysis above, Z_b can be calculated by formula (4). The electromagnetic simulation software CST is applied to extract the impedance of the ''pure'' printed monopole (without the SIHR).

$$Z_c = R + jB \tag{7}$$

where, R and B are the real part and the imaginary part of impedance Z_c, respectively.

According to equivalent circuits in Figure 2, the transformer T converts impedance Z_b to Z_a, we obtain

$$Z_a = n^2 Z_b \tag{8}$$

where, n^2 is the impedance transformer coefficient.

We derive the input impedance Z_{in} from the equivalent circuit in Figure 2 as follows

$$\frac{1}{Z_{in}} = \frac{1}{Z_c} + \frac{1}{Z_a} \tag{9}$$

where, the input impedance Z_{in} can be extracted by simulation software CST, and Z_c can be obtained from formula (7), thus Z_a can be derived from formula (9).

We can get Z_{in}, Z_c, Z_a, and Z_b by simulations and formulas. The specific sizes of the antenna have been shown in Table 1.

The calculated and simulated results of the impedances Z_a, Z_b, Z_c, and Z_{in} are shown in Figure 4. As seen from the Smith impedance chart in Figure 4, the impedance Z_b at the center frequency 3.5 GHz is (230.13-j293.21) Ω. Converted by the transformer T, the impedance Z_a at the same frequency is (187.83-j215.85) Ω. It can be observed that the impedance decrease. At the same time, this trend is observed throughout

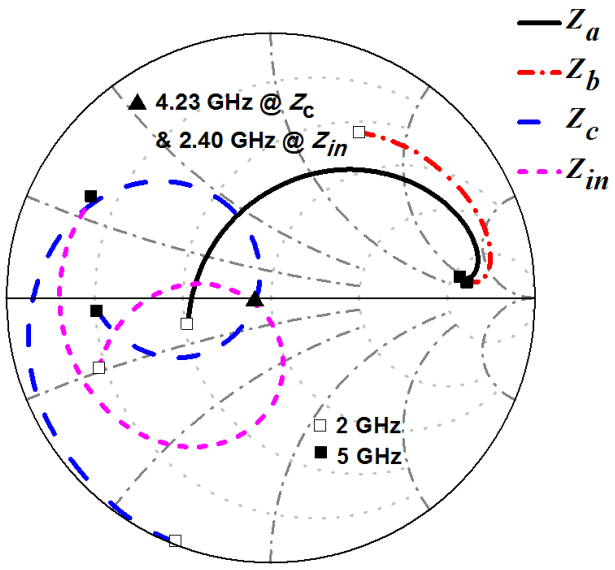

FIGURE 4. Impedance matching procedure of the proposed antenna.

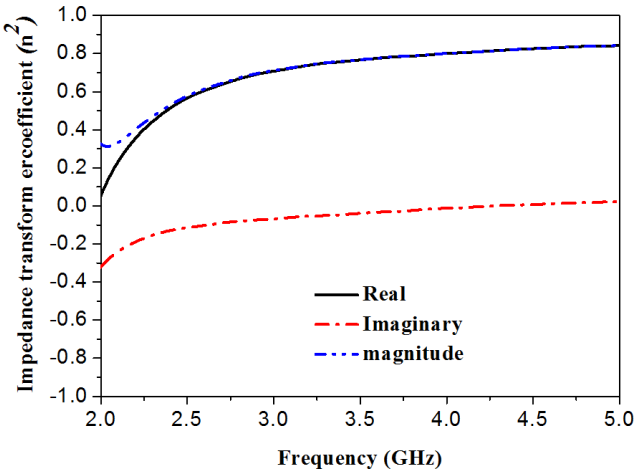

FIGURE 5. The impedance transformer coefficient (n^2).

the frequency band. In addition, in Figure 4, the optimum matching frequency of impedance Z_c (the ''pure'' printed monopole) is 4.23 GHz, and the optimum matching frequency of input impedance Z_{in} is 2.4GHz. Therefore, the resonant frequency is reduced from 4.23 GHz (i.e., 4.23 GHz @ Z_c) to 2.40 GHz (i.e., 4.23 GHz @ Z_{in}), and a printed monopole antenna is realized.

When Z_a and Z_b are determined, the impedance transformer coefficient n^2 can be calculated by formula (8). Figure 5 depicts the calculated result of n^2. So the imaginary part of n^2 is negative, and its magnitude is less than 1. This means that the transformer T is capacitive, and the transformer gradually decreases the impedance.

As described above, the resonant frequency varies with the impedance transformer T [19]. When the size of the NFPR element and monopole is determined, he transformer T will be determined by the thickness H in Figure1.

TABLE 1. Geometric parameter of the proposed printed monopole antenna.

Parameter	Value	Parameter	Value
W	40.00 mm	L_3	4.19 mm
W_A	1.71 mm	S_1	0.40 mm
L	41.50 mm	S_2	0.13 mm
L_A	21.74 mm	S_3	0.25 mm
L_d	8.50 mm	R	24.68 mm
L_1	1.66 mm	θ	64°
L_2	2.07 mm	H	0.508 mm

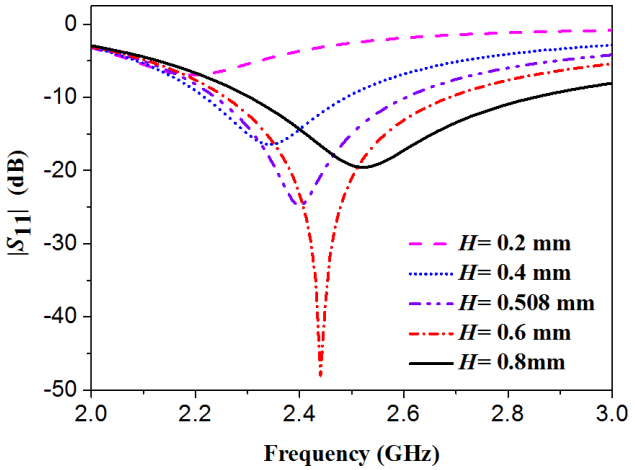

FIGURE 6. The simulated S_{11} varies with H.

Figure 6 shows the simulated effect of different parameters H on the return loss of the antenna, which can be used to tune the resonant frequency of the monopole antenna. Under simulation, the other size parameters are kept in Table 1.

Compared to that of the traditional printed monopole antenna, the resonant frequency of monopole antenna with SIHR is substantially reduced. Meanwhile, it is observed from Figure 6 that the resonant frequency continuously moves to the low frequency with the decreases of the parameter H. That is to say, the stronger the coupling strength between the antenna and the resonator, the lower the resonant frequency of the monopole antenna.

III. MEASURED RESULTS

To verify our design, a sample monopole antenna is fabricated and measured. After optimization carried out by electromagnetic simulation software CST STUDIO SUITE, the width of the microstrip line is as same as that of the monopole antenna. The size of the ground plane is 40.0 mm × 8.5 mm. The specific size of the antenna is shown in Table 1.

The photograph of the antenna is shown in Figure 7. The measurement of the reflection coefficient and radiation pattern has been carried out by Keysight E5071C vector network analyzer and SATIMO near-field antenna measurement system, respectively.

Both the simulated and measured S-parameters are shown in Figure 8. The center frequency of the manufactured antenna is about 2.53 GHz, while the corresponding value of

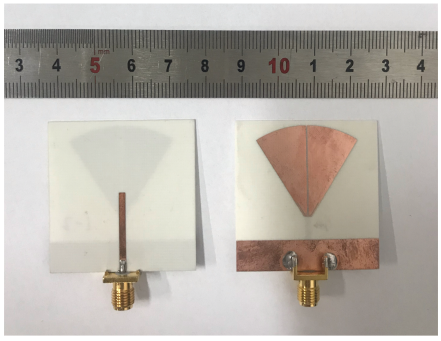

FIGURE 7. Photograph of the proposed printed monopole antenna.

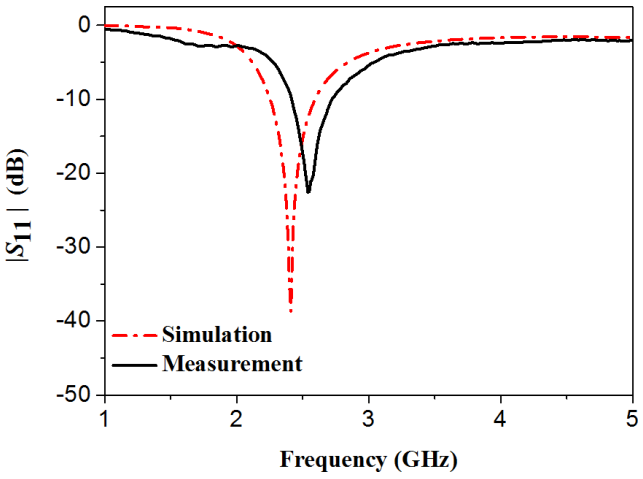

FIGURE 8. Simulated and measured reflection coefficients of the proposed monopole antenna.

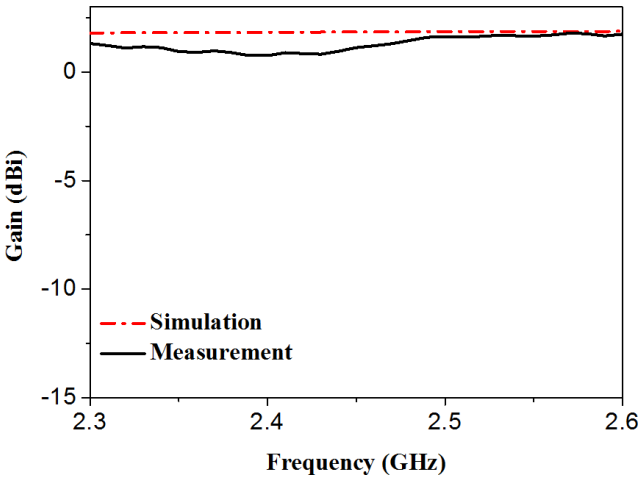

FIGURE 9. Simulated and measured radiation gain of the proposed monopole antenna.

S_{11} at 2.53 GHz is about −20.68 dB. The nuances between the simulation and measurement might be caused by manufacture tolerance.

The simulated and measured gain are shown in Figure 9. The measured results show that the antenna achieves a stable gain over the operating frequency range. The maximum gain is about 2.36 dB, which agree well with the simulated result.

TABLE 2. Comparison of various printed monopole antenna.

Reference	Center Frequency (GHz)	Size (mm^3)	Gain (dB)	Substrate ε_r	FBW (%)
20	2.5	100×60×0.8	3.75	4.4	22.49
21	2.5	46×30×1	2.9	2.65	13.06
22	2.5	40×40×0.8	2.15	4.4	28
23	2.5	20×42.5×0.76	1.9	4.4	13.01
Our work	2.53	40×41.5×0.508	2.36	3.38	13.83

（FBW: Fractional bandwidth）

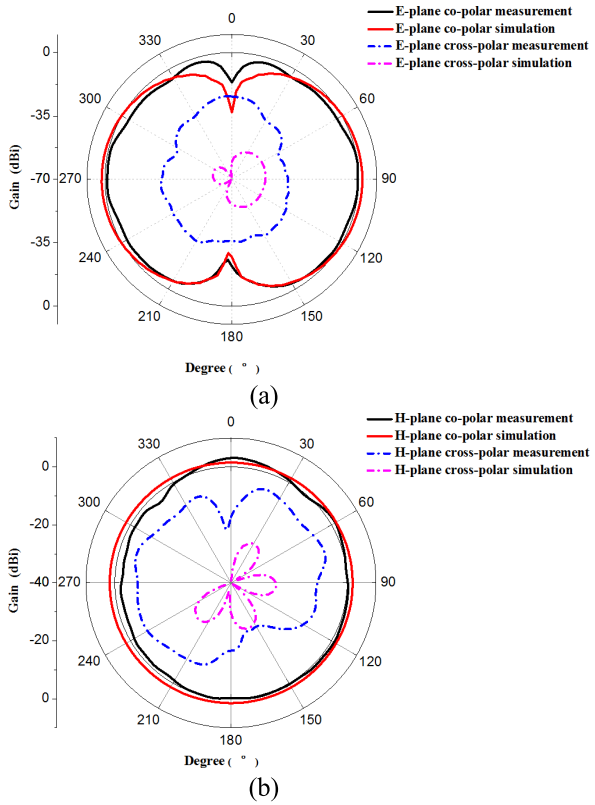

FIGURE 10. Simulated and measured radiation patterns of the proposed antenna at 2.53 GHz (a) E-plane (b) H-plane.

The simulated and measured E-plane and H-plane radiation pattern at 2.53 GHz are given in Figure 10, respectively. As seen from the Figure 10, the antenna has omnidirectional radiation characteristics at the operating frequency.

The proposed printed monopole antenna is also compared with the other reported printed monopole antenna in Table 2.

Compared with the other antennas tabulated in Table 2, the proposed antenna is more compact than [20]. On the other hand, although [22] and [23] are relatively compact, compared with the proposed antenna, the gain is lower, while the FBW of [21] is less than the proposed antenna. Therefore, our proposed printed monopole antenna provides an excellent tradeoff between FBW and gain.

IV. CONCLUSION

This paper presents a novel printed monopole antenna with SIHR loading. By using the coupling between the SIHR element and the driven monopole, the resonant frequency of the antenna can be reduced. Since the resonator is loaded on the back of the driven printed monopole antenna, the radiator size of the antenna is not enlarged. Finally, a prototype antenna is designed, manufactured and measured. The simulated results are in good agreement with the measured results, which provide a good verification for our design method.

REFERENCES

[1] S. Kumar, R. K. Vishwakarma, R. Kumar, and D. Sharma, "A compact printed monopole antenna with symmetrical i and rectangular shaped slots for bluetooth/WLAN/WIMAX applications," in *Proc. Int. Conf. Inf., Commun., Instrum. Control (ICICIC)*, Aug. 2017, pp. 1–5.

[2] M. S. Ellis, A.-R. Ahmed, J. J. Kponyo, J. Nourinia, C. Gbobadi, and B. Mohammadi, "Miniaturised printed monopole antenna with a linked ground plane and radiator," *Electron. Lett.*, vol. 54, no. 11, pp. 676–678, May 2018.

[3] G.-P. Gao, B. Hu, and J.-S. Zhang, "Design of a miniaturization printed circular-slot UWB antenna by the half-cutting method," *IEEE Antennas Wireless Propag. Lett.*, vol. 12, pp. 567–570, 2013.

[4] J. Guo, W. Feng, J.-M. Friedt, Q. Zhao, and M. Sato, "A half-cut compact monopole antenna for SFCW radar-based concrete wall monitoring with a passive cooperative target," *IEEE Geosci. Remote Sens. Lett.*, early access, Sep. 13, 2019, doi: 10.1109/LGRS.2019.2937968.

[5] K.-L. Wong and S.-C. Chen, "Printed single-strip monopole using a chip inductor for penta-band WWAN operation in the mobile phone," *IEEE Trans. Antennas Propag.*, vol. 58, no. 3, pp. 1011–1014, Mar. 2010.

[6] Q. Luo, J. R. Pereira, and H. M. Salgado, "Compact printed monopole antenna with chip inductor for WLAN," *IEEE Antennas Wireless Propag. Lett.*, vol. 10, pp. 880–883, 2011.

[7] L. Guo, S. Wang, X. Chen, and C. G. Parini, "Study of compact antenna for UWB applications," *Electron. Lett.*, vol. 46, no. 2, pp. 115–116, 2010.

[8] R. W. Ziolkowski, "Efficient electrically small antenna facilitated by a near-field resonant parasitic," *IEEE Antennas Wireless Propag. Lett.*, vol. 7, pp. 581–584, May 2008.

[9] M.-C. Tang, R. W. Ziolkowski, S. Xiao, M. Li, and J. Zhang, "Frequency-agile, efficient, near-field resonant parasitic monopole antenna," *IEEE Trans. Antennas Propag.*, vol. 62, no. 3, pp. 1479–1483, Mar. 2014.

[10] V. Jantarachote, S. Chalermwisutkul, K. Schraml, and D. Heberling, "Comparison of meander line and NFRP miniaturization techniques for RFID on-chip antennas," in *Proc. Int. Symp. Antennas Propag. (ISAP)*, Oct. 2017, pp. 1–2.

[11] M.-C. Tang, Y. Duan, Z. Wu, X. Chen, M. Li, and R. W. Ziolkowski, "Pattern reconfigurable, vertically polarized, low-profile, compact, near-field resonant parasitic antenna," *IEEE Trans. Antennas Propag.*, vol. 67, no. 3, pp. 1467–1475, Mar. 2019.

[12] A. Erentok and R. W. Ziolkowski, "Metamaterial-inspired efficient electrically small antennas," *IEEE Trans. Antennas Propag.*, vol. 56, no. 3, pp. 691–707, Mar. 2008.

[13] S. Dakhli, K. Mahdjoubi, H. Rmili, J. M. Floch, and H. Zangar, "Compact, multifunctional, metamaterial-inspired monopole antenna," in *Proc. 6th Eur. Conf. Antennas Propag. (EUCAP)*, Mar. 2012, pp. 1967–1970.

[14] M. Sagawa, K. Takahashi, and M. Makimoto, "Miniaturized hairpin resonator filters and their application to receiver front-end MICs," *IEEE Trans. Microw. Theory Techn.*, vol. 37, no. 12, pp. 1991–1997, Dec. 1989.

[15] X. B. Wei, P. Wang, M. Q. Liu, and Y. Shi, "Compact wide-stopband low-pass filter using stepped impedance hairpin resonator with radial stubs," *Electron. Lett.*, vol. 47, no. 15, pp. 862–863, Aug. 2011.

[16] M. Makimoto and S. Yamashita, "Bandpass filters using parallel coupled stripline stepped impedance resonators," *IEEE Trans. Microw. Theory Techn.*, vol. MTT-28, no. 12, pp. 1413–1417, Dec. 1980.

[17] R. Sorrentino and L. Roselli, "A new simple and accurate formula for microstrip radial stub," *IEEE Microw. Guided Wave Lett.*, vol. 2, no. 12, pp. 480–482, Dec. 1992.

[18] F. Giannini, R. Sorrentino, and J. Vrba, "Planar circuit analysis of microstrip radial stub (short paper)," *IEEE Trans. Microw. Theory Tech.*, vol. 45, no. 7, pp. 1078–1085, Jul. 1997.

[19] P. Jin and R. W. Ziolkowski, "Broadband, efficient, electrically small metamaterial-inspired antennas facilitated by active near-field resonant parasitic elements," *IEEE Trans. Antennas Propag.*, vol. 58, no. 2, pp. 318–327, Feb. 2010.

[20] M.-T. Wu and M.-L. Chuang, "Multibroadband slotted bow-tie monopole antenna," *IEEE Antennas Wireless Propag. Lett.*, vol. 14, pp. 887–890, 2015.

[21] X. Ren, Y. Yin, S. Zheng, S. Zuo, and B. Liu, "Triple-band rectangular ring monopole antenna for WLAN/WiMAX applications," *Microw. Opt. Technol. Lett.*, vol. 53, no. 5, pp. 974–978, May 2011.
[22] H.-W. Liu, C.-H. Ku, and C.-F. Yang, "Novel CPW-fed planar monopole antenna for WiMAX/WLAN applications," *IEEE Antennas Wireless Propag. Lett.*, vol. 9, pp. 240–243, Mar. 2010.
[23] K. G. Thomas and M. Sreenivasan, "A novel triple band printed antenna for WLAN/WiMAX applications," *Microw. Opt. Technol. Lett.*, vol. 51, no. 10, pp. 2481–2485, Oct. 2009.

DONG CHEN (Member, IEEE) received the Ph.D. degree in electronic engineering from the Nanjing University of Posts and Telecommunications, Nanjing, China, in 2010. He has been an Assistant Professor of electromagnetic fields with the Nanjing University of Posts and Telecommunications, since 2014. His current research interests include design of the microwave and RF antenna, transceiver, and power amplifier.

HONGLIN ZHANG (Member, IEEE) received the B.S. degree in telecommunications engineering and the M.S. degree in electrical and information engineering from Hebei University, Baoding, China, in 2005 and 2010, respectively. He is currently pursuing the Ph.D. degree in microelectronics and solid state electronics with the Nanjing University of Posts and Telecommunications, Nanjing, China.

CHUNLAN ZHAO received the B.S. degree in telecommunications engineering from Hebei Polytechnic University, Tangshan, China, in 2008. She is currently with the 13th Research Institute, China Electronic Technology Group Corporation, Shijiazhuang, China.